The GB/SA Continuum Model for Solvation. A Fast Analytical Method for the Calculation of Approximate Born Radii

Di Qiu, Peter S. Shenkin, Frank P. Hollinger, and W. Clark Still*

Department of Chemistry, Columbia University, New York, New York 10027

Received: July 8, 1996; In Final Form: October 7, 1996[⊗]

Atomic Born radii (α) are used in the generalized Born (GB) equation to calculate approximations to the electrical polarization component (G_{pol}) of solvation free energy. We present here a simple analytical formula for calculating Born radii rapidly and with useful accuracy. The new function is based on an atomic pairwise r_{ij}^{-4} treatment and contains several empirically determined parameters that were established by optimization against a data set of >10 000 accurate Born radii computed numerically using the Poisson equation on a diverse group of organic molecules, molecular complexes, oligopeptides, and a small protein. Coupling this new Born radius calculation with the previously described GB/SA solvation treatment provides a fully analytical solvation model that is computationally efficient in comparison with traditional molecular solvent models and also affords first and second derivatives. Tests with the GB/SA model and Born radii calculated with our new analytical function and with the accurate but more time-consuming Poisson−Boltzmann methods indicate that comparable free energies of solventlike dielectric polarization can be obtained using either method and that the resulting GB/SA solvation free energies compare well with the experimental results on small molecules in water.

I. Introduction

The accurate modeling of molecules in solution using molecular mechanics is a challenging problem because solvent is an extended medium having an astronomical number of low-energy states. To treat such a medium in a molecular calculation, both molecular[1−3] and continuum[4−10] models of solvent have been developed. Molecular solvent models employ hundreds or thousands of discrete solvent molecules and provide the most widely used method for carrying out simulations in liquid environments. Though many of the properties of solutions and solutes have been reproduced using calculations employing molecular solvent models, such calculations converge only slowly to precise answers because of the large number of particles and states involved. In fact, molecular solvent calculations generally require several orders of magnitude more CPU time than corresponding gas phase calculations on the same solute. Because molecular solvent models are so computationally demanding, we and others have a significant interest in developing more rapid continuum solvation models. Continuum models treat the solvent as a continuous medium having the average properties of the real solvent and surrounding the solute beginning at or near its van der Waals surface. In principle, such models can provide solvation effects with relatively little computational effort, because the properties of an analytical, continuum solvent are converged by nature and because the model includes no particles other than the atoms of the solute.

A variety of continuum solvation models have been described over the years. Among these, treatments based on surface area or solvent accessible surface area have been recurring themes.[11−13] As a method for evaluating the total solvation free energy (G_{sol}), however, we were concerned that area-based representations would provide poor approximations of the long range electrostatic components of solvation. In particular, purely area-based treatments are problematic in that they give constant solvation energies for all arrangements of ions or other charged atoms having nonintersecting solvent-accessible surfaces. Another popular approach to continuum solvation treats a solute as a distribution of charges or electrical multipoles in a cavity in a dielectric continuum.[14−17] Depending on the model, the cavity may accurately follow the van der Waals surface of the solute or it may be a simple geometrical object such as an ellipsoid that approximates the shape of the solute. These models allow one to compute approximations to a significant (in high dielectric solvents) component of solvation energy, the electrostatic solvent polarization energy (G_{pol}). While such continuum solvation models are computationally efficient, calculating derivatives of G_{pol} with respect to solute atom movement (*e.g.*, for energy minimizations or dynamics calculations) including the effect of cavity boundary fluctuations is computationally intensive and has not been widely used. Furthermore, such dielectric continuum models of the solvent do not include solvent−solvent cavity terms (G_{cav}) or attractive van der Waals solvent−solute interaction terms (G_{vdW}).

Because of the shortcomings of previous models and because we needed a practical solvation model for molecular mechanics and dynamics calculations requiring derivatives, several years ago we developed a new continuum solvation model (termed the GB/SA model) that provided solvation free energies (G_{sol}) based on a generalized Born (GB) treatment of G_{pol} and surface areas (SA) for approximating the cavity and van der Waals contributions to solvation.[9]

In the GB/SA model, the total solvation free energy (G_{sol}) is given as the sum of a solvent−solvent cavity term (G_{cav}), a solute−solvent van der Waals term (G_{vdW}), and a solute−solvent electrostatic polarization term (G_{pol}):

$$G_{sol} = G_{cav} + G_{vdW} + G_{pol} \quad (1)$$

Because saturated hydrocarbons are nonpolar molecules ($G_{pol} \sim 0$) and their G_{sol} in water is approximately linearly related[11−13] to their solvent accessible surface areas (SA), the GB/SA model computes $G_{cav} + G_{vdW}$ together by evaluating solvent-accessible surface areas:[4,5]

[⊗] Abstract published in *Advance ACS Abstracts,* April 1, 1997.

S1089-5639(96)01992-5 CCC: $14.00

$$G_{cav} + G_{vdW} = \sum_{k=1}^{N} \sigma_k SA_k \quad (2)$$

where SA_k (Å^2) is the total solvent-accessible surface area of all atoms of type k and σ_k (kcal/(mol Å^2)) is an empirically determined atomic solvation parameter. For hydrophobic atoms in water and a solvent-accessible surface lying 1.4 Å outside the van der Waals surface, σ has the value of ~0.01 kcal/(mol Å^2). In the work described here, solvent accessible surface areas were computed numerically.

For G_{pol} (kcal/mol), we began with the generalized Born equation and modified it to allow for application to irregularly shaped solutes:

$$G_{pol} = -166.0\left(1 - \frac{1}{\epsilon}\right)\sum_{i=1}^{n}\sum_{j=1}^{n}\frac{q_i q_j}{(r_{ij}^2 + \alpha_{ij}^2 e^{-D_{ij}})^{0.5}} \quad (3)$$

where α_{ij} (Å) $= (\alpha_i\alpha_j)^{0.5}$ and $D_{ij} = r_{ij}^2/(2\alpha_{ij})^2$ and the double sum runs over all pairs of atoms (i and j). α_i is the so-called Born radius of atom i (see below). D_{ij} is the squared ratio of the i,jth atom pair separation to their mean Born diameters, and its exponential is used to force G_{pol} to approximate the dielectric part of Coulomb's law rapidly as atoms i and j move beyond the contact distance of their Born radii. This model has been modified by Truhlar and co-workers and successfully used in conjunction with semiempirical molecular orbital calculations.[10]

Although eq 3 is a simple, pairwise expression, it requires a Born radius (α) for each atom in the solute having an atomic charge (or partial charge). For a simple spherical solute with a charge located at its center (*e.g.*, a model for a metal ion), α can simply be taken as the van der Waals radius of the solute. But for more complex solutes, the Born radius of the ith atom (α_i) depends upon the positions and volumes of all other atoms in the solute because they displace the solventlike dielectric medium. The Born radius of a charged particle is actually not so much a radius as it is a kind of average distance from the atomic charge to the boundary of the dielectric medium. For certain simple systems, the value of α is thus obvious. For example, α for an atom at the center of a spherical macromolecule would be the radius of the macromolecule. For systems having irregular shapes, however, α is more complicated to evaluate. In previous descriptions of the GB/SA model, α for such solutes has been obtained by a numerical, finite difference method based on the Born equation.[9] While this numerical evaluation provided well-defined and reasonably accurate evaluations of α's, it was also the most time-consuming part of the GB/SA solvation calculation (eq 3). Furthermore, because of the numerical nature of the previous α evaluation, full derivatives of G_{pol} were not readily obtained.

In this paper, we describe a significant enhancement to the GB/SA solvation model in the form of a fast, analytical approach to computing atomic Born radii. Though our analytical approach to α is not exact, we show here that it yields Born radii that compare reasonably well with accurate α's calculated numerically. Furthermore, in conjunction with the GB/SA model for water, experimental solvation energies are well reproduced by GB/SA calculations using α's computed either by our rapid approximate method or by a slower but accurate numerical method. Because the new approach to computing Born radii makes the GB/SA solvation model fully analytical, we implemented it several years ago with full first and second derivatives as an unpublished feature in our molecular modeling program MacroModel/BatchMin.[18] In this paper, we describe our analytical approach to Born radii in detail, reoptimize the parameters associated with the model based on Poisson equation derived G_{pol} energies, and show how the model performs in reproducing accurate Born radii and experimental solvation energies. We also compare its performance to a different approach to Born radii recently described by Hawkins *et al.*[19]

II. Methods

To define our approach to computing Born radii (α), we begin with the original Born expression (eq 4) for a monoatomic spherical ion surrounded by a continuum dielectric medium

$$G_{pol} = -166.0\left(1 - \frac{1}{\epsilon}\right)\frac{q^2}{\alpha} \quad (4)$$

representing a solvent which relates the total dielectric polarization energy of the system (G_{pol}, kcal/mol) to the charge (q, electrons), the dielectric constant (ϵ) of the medium, and α, the ion's effective or Born radius (or, more precisely, the distance from the center of the ion to the boundary of the dielectric, Å). For such a spherical system in a solventlike, continuum dielectric medium, the effective dielectric boundary will be found at some fixed distance (previously defined[9] as the dielectric offset distance ϕ) from the van der Waals surface of the solute. Thus, for a spherical monoatomic solute, there is a simple relationship between α and the distance from the ion center to its van der Waals surface ($\alpha = \phi + R_{vdW}$). For a polyatomic solute, however, the corresponding distance from an atomic charge to the molecular van der Waals surface will vary depending on which part of the molecular surface is being considered. To avoid the mathematical complexities associated with such an angularly dependent α, we sought an appropriate way to average the various distances from a given charge to all points on the dielectric boundary to produce a single value of α for use in eq 3.

The approach we developed begins with eq 4 and the following idea. Imagine a polyatomic solute whose atoms are all electrically neutral but displace the dielectric solvent medium to create a solute-shaped cavity in the medium. For such a system, $G_{pol} = 0$. Now, choose an atom (i) and place an electrical charge (q_i) on it. The resulting system will now have some nonzero G_{pol}. If we could compute this G_{pol}, we could then use eq 4 to calculate α_i, a value corresponding to a spherically averaged, effective Born radius of atom i. Thus, given a method to calculate G_{pol} for a system consisting of a continuum dielectric and an irregularly shaped solute with a single charge located at any position within the solute, Born radii for each atom in the solute could be readily calculated. This general approach to Born radii was introduced as part of the original GB/SA solvation model and assumes that the Born radius of a given atom does not depend upon the charge distribution in the system.[9] The following paragraphs describe a method for carrying out such G_{pol} calculations in the context of a solute having atom-centered charges in a continuum dielectric medium. We begin by describing our analytical method for the rapid calculation of such G_{pol}'s and thus Born radii.

An Analytical Approach to Born Radii (α). In order to compute α efficiently, we sought an analytical function leading to usefully accurate Born radii via a simple pairwise evaluation of the atoms in a molecular solute. The idea we developed is best described with the aid of Figure 1. Imagine that we wish to compute α_i in a polyatomic solute in a solvent represented by a continuum dielectric. All of the atoms of the solute may be considered to displace any dielectric within their van der Waals surfaces to create a solute-shaped cavity in the solventlike

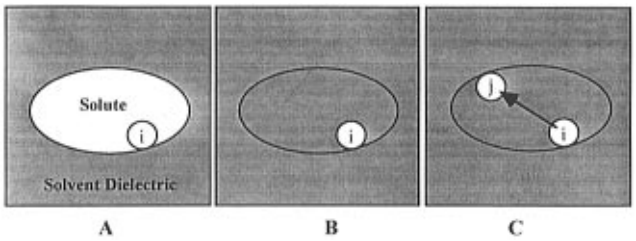

Figure 1. V/r^4 model for evaluating the Born radius of atom i in a solute (see text).

dielectric medium as indicated in Figure 1A. In order to calculate α_i, we compute $G_{\mathrm{pol},i}$ for a simplified system in which all atoms in the solute except for i are electrically neutral as outlined above. To compute $G_{\mathrm{pol},i}$, we start by removing all the atoms in the solute except atom i (Figure 1B). The $G_{\mathrm{pol},i}$ energy of that system would be simply given by the Born equation (eq 4), with α equal to atom i's van der Waals radius (plus any ϕ). Now consider the effect on the system of including one of the solute's other atoms (*e.g.*, atom j, Figure 1C). While atom j is uncharged, it changes $G_{\mathrm{pol},i}$ because it displaces a piece of dielectric medium equivalent to its volume (V_j). The inclusion of atom j thus results in an increase of the energy of the system ($G_{\mathrm{pol},i}$ becomes less negative) which is proportional to V_j and inversely proportional to the distance between atoms i and j (r_{ij}) raised to the fourth power.[20] This V_j/r_{ij}^4 relationship follows from the loss of a classical charge/induced dipole interaction between the charge on atom i and the dielectric medium that is displaced by atom j. By similarly including the effects of dielectric displacement by all other atoms in the solute, $G_{\mathrm{pol},i}$ for the full solute system (approximately Figure1A) could be computed and its reciprocal would yield α_i via eq 4.

Though the above model for computing $G_{\mathrm{pol},i}$ is reasonable, it is also simplistic in that it defines the solvent dielectric as occupying all regions of space outside the van der Waals envelopes of the individual atoms of the solute. In reality, however, a molecular solute in molecular solvent includes numerous small voids between solute atoms that are too small to be filled by solvent molecules. Furthermore, there may be overlaps of certain atomic volumes. Finally, the V_j/r_{ij}^4 relationship is accurate only when atoms i and j are widely separated (r_{ij} is large). While such defects in our model could be corrected, we thought that the basic model might capture the essential physics of the system and thus be useful for rapidly computing approximate Born radii. We added a series of empirical scaling parameters to the basic V/r^4 equation in an attempt to minimize the effect of model defects in an average sort of way. We then optimized the values of these scaling parameters (P_1−P_5) to best reproduce accurate $G_{\mathrm{pol},i}$ for the atoms in a diverse set of molecules. The explicit equation we use is given as eq 5a and yields $G'_{\mathrm{pol},i}$, a polarization energy that assumes a unit charge on atom i and a surrounding medium of high dielectric ($1 - 1/\epsilon \approx 1.0$):

$$G'_{\mathrm{pol},i} = \frac{G_{\mathrm{pol},i}}{1-\frac{1}{\epsilon}} = \frac{-166.0}{R_{\mathrm{vdW}-i} + \phi + P_1} + \sum^{\mathrm{stretch}} \frac{P_2 V_j}{r_{ij}^4} + \sum^{\mathrm{bend}} \frac{P_3 V_j}{r_{ij}^4} + \sum^{\mathrm{nonbonded}} \frac{P_4 V_j \mathrm{CCF}}{r_{ij}^4} \quad (5a)$$

where $G_{\mathrm{pol},i}$ = polarization energy of atom i (kcal/mol), ϕ = dielectric offset (Å), r_{ij} = distance between atoms i and j (Å), V_j = volume of atom j (Å^3), $R_{\mathrm{vdW}-i}$ = van der Waals radius of atom i (Å), P_1 = single-atom scaling factor, P_2 = 1,2 scaling factor, P_3 = 1,3 scaling factor, P_4 = 1,≥4 scaling factor, P_5 = soft cutoff parameter, and CCF = close contact function for 1,≥4 interactions where

$$\mathrm{CCF} = 1.0 \quad \text{if} \quad \left(\frac{r_{ij}}{R_{\mathrm{vdw}-i} + R_{\mathrm{vd}-j}}\right)^2 > \frac{1}{P_5}$$

otherwise

$$\mathrm{CCF} = \left\{0.5\left[1.0 - \cos\left\{\left(\frac{r_{ij}}{R_{\mathrm{vdw}-i} + R_{\mathrm{vdW}-j}}\right)^2 P_5 \pi\right\}\right]\right\}^2$$

Making the same assumptions regarding the charge on atom i and dielectric constant of the medium, we can then use the simplified Born equation (5b) to compute α_i:

$$\alpha_i = -\frac{-166.0}{G'_{\mathrm{pol},i}} \quad (5b)$$

The right-hand side of eq 5a defines G'_{pol} and depends on neither ϵ nor the charge distrubution. α_i (eq 5b) depends on G'_{pol} only and is therefore also independent of ϵ and the charge distribution. The first equality in eq 5a shows that G'_{pol} may be interpreted as the infinite-dielectric limit of G_{pol}.

The first term in eq 5a gives the Born energy of atom i alone in the dielectric medium (as in Figure 1B). The remaining three terms take into account the effect of all other atoms (atoms j in Figure 1C) which make the magnitude of $G_{\mathrm{pol},i}$ smaller by displacing the dielectric medium. We distinguish these other atoms by their connectivity to atom i. Thus, atoms involved in 1,2-stretching interactions with atom i are treated differently from those involved in 1,3-bends or nonbonded (1,≥4) interactions. We made this distinction because we expected our simple pairwise model to show deviations from a real molecular system that depended systematically on the separation of the atom pairs (*e.g.*, covalent bound atoms (1,2-stretching interactions) would be expected to be systematically more overlapping than any other pairs of atoms). The separation of atomic pairs into classes corresponding to stretch, bend, and nonbonded categories, which correlate with increasing pair separation and geometrical disposition, also allows the scaling parameters to accommodate systematic deviation from ideal V/r^4 behavior as r increases. The only deviation of our model from the scaled V/r^4 treatment occurs when nonbonded atom pairs come within 80% of their summed van der Waals radii and thus overlap significantly. In that situation, the CCF is used to reduce the effective volumes of the overlapping atoms.

Associated with eq 5a are several details of implementation that improve the model's efficiency and are justified by the facts that bond lengths and bond angles do not vary greatly among different conformations of the same molecule. Thus, for j atoms involved with atom i in stretching (term 2 in eq 5a) and bending interactions (term 3 in eq 5a), we take equilibrium bond lengths and angles from the molecular mechanics force-field stretch and bend parameters to define r_{ij} rigidly for those terms. Thus, all terms in eq 5a can be taken as constants (connectivity dependent but coordinate independent) for a given molecule except for the last term which deals with the effects of nonbonded atoms. This simplification allows the contributions of 1,2- and 1,3-atom pairs to α to be computed once at the beginning of an energy minimization or molecular simulation and then used as constants throughout the rest of the calculation.

For atomic volumes (V_j) in eq 5a, we use simple atomic volumes minus those subvolumes that would lie inside directly bonded atoms (k). Thus, given constant bond lengths, V_j is also

a constant and is thus given by

$$V_j = \frac{4}{3}\pi R_{\mathrm{vdW}-j}{}^3 - \sum_k \frac{1}{3}\pi h_{jk}{}^2(3R_{\mathrm{vdW}-j} - h_{jk}) \qquad (6)$$

where h_{jk} is the difference between $R_{\mathrm{vdW}-j}$ and the vector from the center of atom j to the center of the circle formed by the intersection of the overlapping spheres.

$$h_{jk} = R_{\mathrm{vdW}-j}\left(1 + \frac{R_{\mathrm{vdW}-k}{}^2 - R_{\mathrm{vdW}-j}{}^2 - r_{jk}{}^2}{2R_{\mathrm{vdW}-j}r_{jk}}\right)$$

For van der Waals radii, we use atomic radii taken as 0.5σ from the Jorgensen OPLS force field[21] except for hydrogens to which we assign a radius of 1.15 Å as described previously.[9] Given our rigid treatment of atoms directly bonded to atom i, the distance between bound atoms j and k (r_{jk}) is also a constant which we define to be $1.01l_0$, where l_0 is the natural length of that bond as given by the molecular mechanics force field in use. The 1% increase in l_0 allows for the minor stretching of bonds that commonly accompany energy minimization.

In tests on small molecules, we find the assumptions of constant bond lengths and angles (using natural lengths and angles from a standard molecular mechanics force field) to change the total solvation energies by <1% in comparison with solvation energies having 1,2 (stretching) and 1,3 (bending) terms computed from actual, energy-minimized atomic coordinates.

One further simplification was made to improve the model's efficiency, and that entails using the united-atom approximation for the hydrocarbon portions of the solute. The united-atom approximation is common in the modeling of large molecules and involves substitution of carbons and all directly bound hydrogens with single, enlarged superatoms. The justification of the united-atom approach is that hydrogens are relatively small atoms and lie mostly within the van der Waals envelope of attached carbons. In eq 5a, this approximation significantly reduces the number of j atoms that have an effect on the Born radius of atom i by eliminating the effect of all hydrogens bound to carbon and instead using the appropriate united-atom radius for these carbons.

To determine the best values for parameters P_1-P_5 in eq 5a, we first computed a large number of atomic Born radii using the Poisson−Boltzmann (PB) equation as implemented in the DelPhi program of Honig *et al.*[15−17] DelPhi is widely regarded as a reliable predictor of electrostatic interactions in polar solvents and has been successful in computing good approximations to the electrostatic component of hydration energies.[22] The program uses a finite difference method to iteratively solve the PB equation (FDPB) for a charge-bearing molecular solute in a continuum dielectric medium and thus provides a method for computing accurate G_{pol} energies assuming atom-centered solute charges and a dielectric continuum surrounding the solute. In our calculations, the ionic strength was set to zero so we actually used DelPhi to solve the Poisson equation.

Given the FDPB approach to computing G_{pol} and its relationship with α (eq 4), it is possible (though time-consuming) to compute accurate Born radii for all atoms in virtually any molecule in a solventlike, continuum dielectric medium. Thus, to compute the Born radius for atom i in a molecule, one places a unit charge on that atom ($q_i = 1.0$) and sets the charges of all the other atoms in the molecule to zero. DelPhi is then used to compute the polarization energy of the system ($G_{\mathrm{pol},i}$) with a solute dielectric constant of 1.0, a solution ionic strength of 0.0, and a water-like continuum dielectric medium ($\epsilon = 80$) starting at the van der Waals boundary of the solute. The same OPLS-derived van der Waals radii were used in these FDPB calculations as were used with eq 5a (see above). Applying Born eq 4 to the $G_{\mathrm{pol},i}$ thus calculated gives the Born radius of atom i (α_i). To the extent that DelPhi's FDPB calculation is accurate, α_i will also be accurate.

We use an internal dielectric constant of 1, rather than a value in the range 2-4, as used by Honig and co-workers,[15−17] because the Born equation (eq 3) we are using assumes an internal dielectric constant of 1. This value for ϵ has been shown to be appropriate when considering the solvation energies of small molecules.[23]

We optimized the parameters P_1-P_5 in eq 5a to minimize the discrepancy between Born radii determined by the above FDPB method and by eq 5a. We first assembled a data set of 189 representative organic molecules and biopolymers containing more than 10 000 atoms (see supporting information). These structures included both all-atom and united-atom (hydrocarbon fragments only) representations of the molecules. All molecules in the data set were first energy minimized *in vacuo* using the MacroModel AMBER* force field.[25] Next we used the above FDPB method and eq 4 to evaluate an accurate Born radius for each atom in every molecule in the data set. Our parameter optimization procedure used a simulated annealing algorithm combined with the downhill Simplex method[26] that randomly varied P_1-P_5 to minimize an error function (eq 7) comparing results from FDPB and eq 5a.

Our error function (eq 7) was defined as the average squared difference between atomic polarization energies ($G'_{\mathrm{pol},i}$) computed by FDPB and eq 5a for all atoms in the data set. We based our error function on $G'_{\mathrm{pol},i}$ instead of the corresponding α_i because we are more interested in reproducing polarization energies than Born radii *per se*. This choice of ERROR biased the optimization procedure toward atoms having smaller Born radii, thus making it more sensitive to those atoms making the largest contributions to dielectric polarization energies.

$$\mathrm{ERROR} = \sqrt{\frac{\sum_{i=1}^{N}(G'_{\mathrm{pol},i}\,(\mathrm{eq\ 5a^*}) - G'_{\mathrm{pol},i}(\mathrm{FDPB}))^2}{N}} \qquad (7)$$

N is the total number of atoms in the data set (here 10 034) and $G'_{\mathrm{pol},i}$ indicates the atomic polarization energies based on an atomic charge (q_i) of 1.0 and medium dielectric constant of 80.

After optimization of P_1 through P_5, the value of ERROR (eq 7) was 7.9 kcal/mol. This value of ERROR corresponds approximately to a 3% average error in $G'_{\mathrm{pol}-i}$ for atoms in these ionic model systems. Analyzing the Born radii calculated by parameterized equations (5a) and (5b) for the entire data set, we found that Born radii for certain atom types were consistently too small relative to accurate Born radii from FDPB calculations (see Table 1, column eq 5a). These atoms were S, Cl, N(sp^2), N(sp^3), H(N), and H(O). We therefore increased the van der Waals radii of these atom types by 5% except for S whose radius was increased by 10%. Reoptimization of P_1 through P_5 using these altered radii in eq 5a then led to ERROR = 6.9 kcal/mol, and the results are summarized in Table 1, column eq 5a*. The final values for these parameters are

P_1	0.073
P_2	0.921
P_3	6.211
P_4	15.236
P_5	1.254

TABLE 1: Average Errors in Born Radii (α) Based on Atom Type

atom	MacroModel atom type	av error = α − α(FDPB), Å: eq 5a[a]	av error = α − α(FDPB), Å: eq 5a*[b]	no. atoms[c]
C(sp)	C1	−0.028	0.002	1
C(sp^2)	C2	0.024	0.070	1668
C(sp^3)	C3	−0.135	−0.102	723
CH(sp^3)	CA	−0.043	0.015	727
CH_2(sp^3)	CB	0.062	0.096	597
CH_3(sp^3)	CC	0.145	0.180	393
CH(sp^2)	CD	0.096	0.132	245
O(sp^2)	O2	−0.099	−0.066	940
O(sp^3)	O3	−0.138	−0.097	331
O^-	OM	0.001	0.029	209
N(sp)	N1	−0.011	0.015	1
N(sp^2)	N2	−0.249	0.014	876
N(sp^3)	N3	−0.406	−0.225	14
N^+(sp^2)	N4	0.119	0.153	69
N^+(sp^3)	N5	−0.048	−0.018	86
H(C)	H1	−0.069	−0.051	1638
H(O)	H2	−0.187	−0.072	232
H(N)	H3	−0.564	−0.410	857
H(N^+)	H4	−0.023	0.000	365
S	S1	−0.574	−0.241	35
P	P0	−0.128	−0.099	17
F	F0	−0.112	−0.099	17
Cl	Cl	−0.285	−0.120	17
Br	Br	−0.030	0.001	1
I	I0	−0.024	0.007	4

[a] By V/r^4 model (eq 5) using OPLS radii and 1.15 Å for H. [b] V/r^4 model (eq 5) using OPLS radii and 1.15 Å for H except that N(sp^2), N(sp^3), H(O), H(N), and Cl are enlarged by 5% and S is enlarged by 10% (see text). [c] Number of atoms in data set of designated atom type.

While the work described here was underway, a different pairwise approach for the evaluation of Born radii was reported by Hawkins *et al.*[19] Their method was based on our original finite difference Born shell approach to Born radii but employed a pairwise descreening approximation[27] to make the approach both rapid and analytical. We term this method the PDA method. The PDA method is similar in spirit to our V/r^4 method (eq 5a) in that it computes an atom's Born radius by summing the effects of dielectric displacement by all other atoms in the molecule. Though both methods approach the Born radius problem using an atomic pairwise algorithm, the basic underlying models differ in that the PDA method is an analytical approximation to our original Born shell model,[9] whereas our new work is based on the V/r^4 model of Figure 1. To see how the PDA method performs relative to eq 5a and accurate FDPB results, we programmed and tested the Hawkins formula for α^{-1}.

Like our V/r^4 model, the PDA approach is simplistic in that it does not explicitly deal with voids between atoms or atomic overlaps. Instead, empirical scaling factors (S_x) are used to adjust the atomic radii to minimize such effects. These scaling factors were optimized to best reproduce known solvation energies of more than 100 organic molecules using a GB/SA-like solvation model with SM2 atomic radii and AM1-derived partial charges. Their values as given by Hawkins *et al.* are shown below under the S_x column:

atom	S_x	S_x*
H	0.82	0.78
C	0.70	0.77
O	0.54	0.64
N	0.66	0.66

In comparing the results from the PDA method with those from our V/r^4 method (eq 5a) and FDPB, we used Hawkins *et al.*'s original scaling factors (S_x) as well as modified scaling parameters (S_x*) that we optimized to minimize the same error function (eq 7) and data set used to optimize P_1 through P_5. These modified scaling parameters should be more appropriate for the OPLS atomic radii and charges used here. We term the results of the PDA method with our modified S_x* scaling factors as the PDA* results in the discussion below. For compounds containing sulfur, phosphorus, or halogens, no PDA or PDA* calculations were carried out because scaling parameters were unavailable for those atom types.

III. Results and Discussion

In the following sections, we test the ability of our V/r^4 model (eq 5a) to reproduce solventlike, continuum dielectric polarization energies (atomic $G'_{pol,i}$ and molecular G_{pol}) from FDPB calculations. We also use V/r^4 and FDPB-derived Born radii in our GB/SA solvation model to compute the total solvation energies (G_{sol}) of small molecules in water where experimental data are available. Finally, we provide similar comparisons using the PDA approach to Born radii.

IIIa. Comparison with Finite Difference Poisson−Boltzmann (FDPB) Results. Because solution of the Poisson equation provides polarization energies for charge-bearing objects in a continuum dielectric medium, it provides a convenient source of accurate $G'_{pol,i}$ data for comparison with corresponding energies calculated using the V/r^4 model (eq 5a). This comparison for all 10 034 atoms in our data base is shown graphically in Figure 2A. To make the correlation graphs easier to read, we have plotted $G'_{pol,i}$ for small molecules and large molecules (various nonapeptide conformations and crambin) separately. As these graphs show, the V/r^4 model does the best job at reproducing FDPB atomic polarization energies for those atoms having the largest (most negative) solvent polarization energies. Those atoms are the ones having the smallest Born radii. Thus, the atoms making the largest contributions to solvent polarization energies are most accurately treated. While most atoms had solvent polarization energies that were within a few percent of the correct FDPB results, a significant number of atoms having larger Born radii (less negative $G'_{pol,i}$) had Born radii that were systematically smaller than those from the FDPB calculations. These outliers occurred primarily in the larger molecules and tended to be those atoms most deeply buried within a solute.

In the FDPB method, a Connolly surface is used to define the solute boundary and to exclude dielectric from small voids in regions of densely packed solute atoms. In contrast, the V/r^4 model uses atomic van der Waals surfaces to define those volumes from which the dielectric is excluded. This approach effectively leaves small, interstitial void volumes containing dielectric within the solute. While the parameterization described above minimizes such differences in an average way, differences still remain, especially for deeply buried atoms in large molecules. The net effect is that these atoms often experience a higher microdielectric environment in the V/r^4 model than in the FDPB treatment.

Table 2, column eq 5a*, provides statistical data on the correlation between eq 5a and FDPB calculations of atomic medium polarization energies. Given there are correlation coefficients (r) for a linear fit between $G'_{pol,i}$ computed by the two methods. Atomic polarization energies for small molecules are better reproduced ($r = 0.96$) than those of large molecules ($r = 0.92$), as expected given our systematic overestimation of $G'_{pol,i}$ for buried atoms. The average unsigned error in $G'_{pol,i}$ for all 10 034 atoms in our data set is 4.27 kcal/(mol atom) (just under 6% of the mean atomic polarization energy).

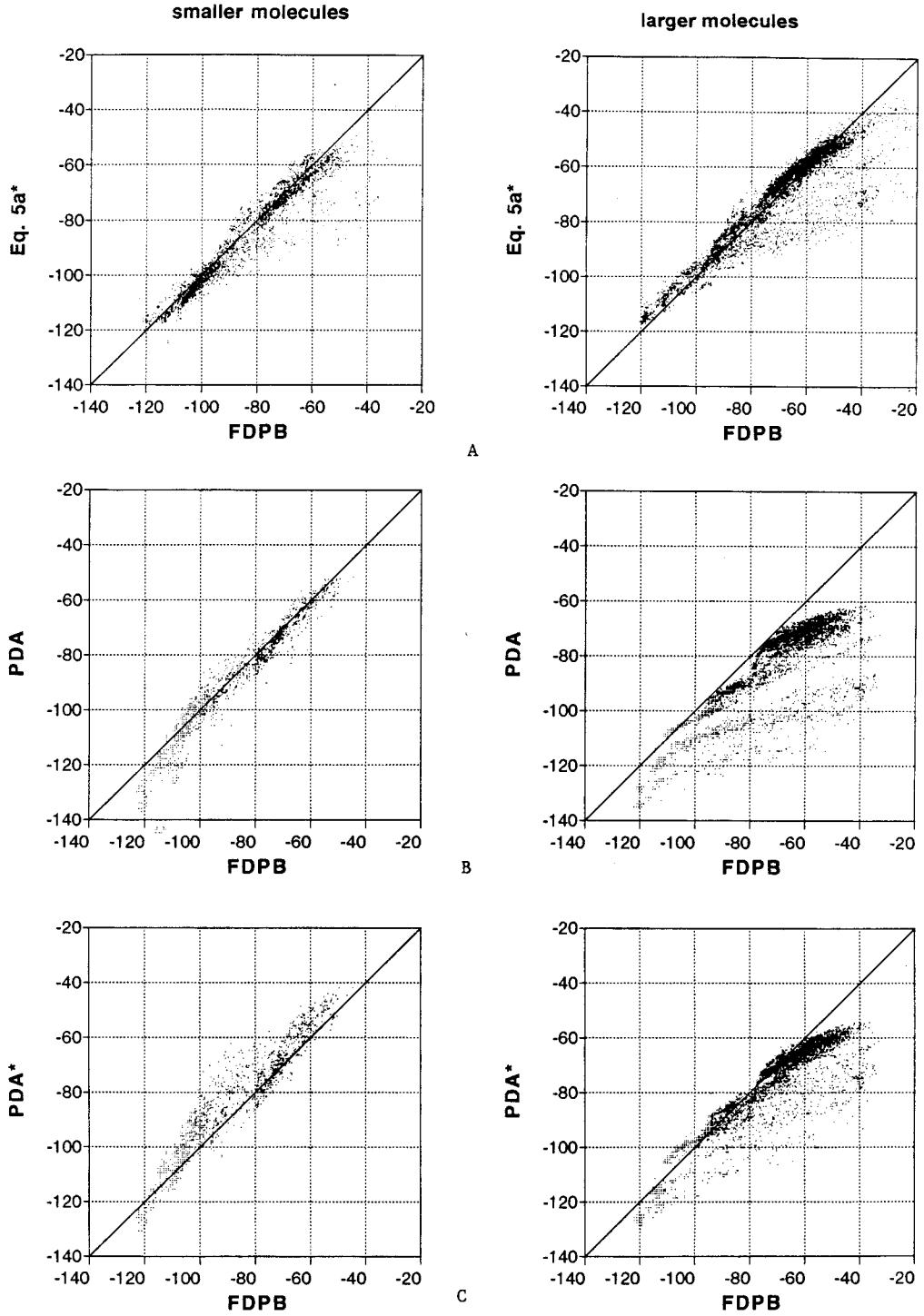

Figure 2. Comparison of atomic dielectric medium polarization energies ($G'_{pol,i}$, kcal/(mol atom)) computed by various methods. Panel A: GB radii from eq 5a with optimal atomic radii. Panel B: GB radii using the method of ref 19. Panel C: GB radii using method of ref 19 with reoptimized S_x parameters.

Also given in Table 2 (eq 5a* column) are Born radius data computed from $G'_{pol,i}$ (eq 5b) for the same 10 034 atoms. The correlation between these V/r^4- and FDPB-derived Born radii is weaker ($r = 0.85$) than with the energetic equivalent $G'_{pol,i}$, and the average unsigned error in Born radii over the entire set is 0.17 Å/atom. As discussed above, the greatest differences in Born radii are found with those atoms having the largest Born radii. These effectively larger atoms contribute the least to the solvation energies so that the overall V/r^4-derived and FDPB energetic results still agree reasonably well, as we show below.

We next investigated the agreement between GB and FDPB in computing solventlike dielectric medium ($\epsilon = 80$) polarization energies (G_{pol}) for molecules bearing complete sets of atomic charges. The same charge sets were used in both calculations and came from the AMBER* force field.[25] The molecules were the same 189 organic and biological molecules used in the above $G'_{pol,i}$ and α_i calculations. The G_{pol} comparison in which the GB calculations employed V/r^4-derived Born radii is shown in Figure 3A. There is a strong linear correlation (slope = 1.000, correlation coefficient = 0.999) between the two G_{pol} calculation results. The differences that do exist are generally small relative to the total solvation energies involved and are explicitly plotted next to the correlation graph. The molecule having the largest difference in G_{pol} energy as calculated by the GB method with

TABLE 2: Comparison of Atomic Polarization Energies ($G'_{pol,i}$, kcal/mol) and Born Radii (α_i, Å) Calculated by Various Methods and Compared to Poisson−Boltzmann Results[a]

polarization energies	FDPB[b]	eq 5a*[c]	PDA[d]	PDA*[e]
mean energy per atom	−76.7	−77.6	−85.7	−78.4
slope (small mols)[f]		0.93	1.01	0.97
corr (small mols)[g]		0.96	0.97	0.95
slope (large mols)[f]		0.83	0.74	0.78
corr (large mols)[g]		0.92	0.83	0.90
av unsigned error		4.27	9.40	5.89

Born radii	FDPB[b]	eq 5*[c]	PDA[d]	PDA*[e]
mean α	2.33	2.27	2.01	2.18
slope[f]		0.64	0.46	0.75
corr[g]		0.85	0.58	0.82
av unsigned error		0.17	0.31	0.21

[a] Data computed for 10 034 atoms in 189 molecules bearing single-unit charges ($q_i = 1$) and in an external dielectric continuum with $\epsilon = 80$ except for PDA and PDA* results which are based on 7407 atoms in 139 molecules (see text). [b] Accurate result given by finite difference Poisson−Boltzmann calculation. [c] V/r^4 model (eq 5). [d] Pairwise descreening approximation method of Hawkins *et al.*[19] ($G'_{pol,i} = -166\alpha_i^{-1}$). [e] Pairwise descreening approximation method with S_x*-modified scaling parameters (see text). [f] Slope of linear fit between designated method and FDPB. [g] Correlation coefficient for linear fit of points between designated method and FDPB.

V/r^4 Born radii is the protein crambin, the largest molecule in the data set. Even here the +16 kcal/mol GB/FDPB difference is relatively small: about 7% of crambin's total dielectric polarization energy. The average unsigned error of GB(V/r^4) G_{pol} relative to FDPB for all 189 molecules in the data set is 1.93 kcal/mol.

Because the above molecular GB G_{pol} calculations depend both upon the validity of the GB equation (eq 3) and of the V/r^4 model (eq 5), we carried out one further test to probe the sensitivity of these G_{pol} calculations to the above-noted errors in V/r^4-derived Born radii. This test involved using accurate, FDPB-derived Born radii in the GB equation. The results are plotted in Figure 3B and indicate the best G_{pol} results that the GB equation (3) can provide relative to full G_{pol} calculations by the FDPB method. While the errors in molecular G_{pol} are generally smaller with FDPB-derived Born radii, the improvement is not dramatic and the average unsigned error for the entire data set is now 1.74 kcal/mol.

IIIb. Comparison with Experimental Free Energies of Solvation in Water. While the above comparisons with Poisson−Boltzmann calculations support the utility of the GB and V/r^4 approximations in computing polarization energies (G_{pol}) for a molecular solute in a dielectric continuum medium, the medium in real-world applications of the method is not a dielectric continuum but a real molecular solvent. We therefore ask how well GB calculations using various sources of Born radii reproduce actual solvation free energies for the polar solvent water. Here, accurate experimental data are more limited and are available only for certain small molecules. To compare our calculations with experiment, we chose 36 small organic molecules having diverse functional groups and whose hydration free energies appeared accurately known.[28] As in the original GB/SA work,[9] we also limited the molecules to those bearing functional groups having atomic partial charges defined by Jorgensen's OPLS force field[21] or derived from electrostatic potential fitting to minimally HF/6-31G* *ab initio* wave functions.

To calculate the total solvation free energies of these molecules, we used the GB/SA solvation model (eqs 1−3) using Born radii calculated using the methods described above. In the original GB/SA work,[9] all atoms were treated as hydrophobic and used the same atomic solvation parameter ($\sigma = 7$ cal/(mol Å^2)) in the solvent-accessible surface area (SA) part of the model. Since that time, we have adopted Cramer and Truhlar's approach[19] of using different σ's for different atom types though we distinguish only a few atom types in this way. Thus, we treat atoms based on their approximate hydrophobicity/hydrophilicity and use the following three area-based atomic solvation parameters for the common atom types: σ(C(sp^3), S) = 10 cal/(mol Å^2), σ(C(sp^2), C(sp), P) = 7 cal/(mol Å^2), σ(O, N) = 0 cal/(mol Å^2). To speed our surface area calculations, we employ the united atom approximation in the SA part of the GB/SA model, and thus, σ(H) is zero.

The results of our GB/SA hydration free energy (G_{sol}) calculations are summarized along with experimental data in Table 3. Results using our V/r^4 Born radius model are given in column eq 5a* and plotted in Figure 4. There it can be seen that GB/SA(α from V/r^4) solvation energies are strongly correlated with experiment (average unsigned error 0.9 kcal/mol, linear fit slope = 0.96, $r = 0.94$). We also carried out analogous GB/SA calculations using accurate, FDPB-derived Born radii. Those data are shown in the FDPB column of Table 3 and have an average unsigned error of 0.8 kcal/mol. Thus, comparable accuracy relative to experiment is obtained in our GB/SA G_{sol} calculations regardless of the source of the Born radii. The utility of the V/r^4 model for computing Born radii for use in the GB/SA solvation model would therefore seem to be validated.

Finally, we tested the basic GB equation (eq 3) of our GB/SA model for solvation by replacing the entire GB equation with a full FDPB calculation of G_{pol}. Those results are given in Table 3 under the FDPB/SA column and yield an average unsigned error of 0.9 kcal/mol relative to experiment. Thus, to the extent that experiment is the best yardstick for assessing the usefulness of a model in real applications, we find no evidence that the FDPB method is any better than the simpler GB approximation. Indeed, we think it likely that the approximation of a polar molecular solvent by a simple continuum dielectric is more significant than the difference between FDPB and GB approaches to G_{pol}.

IIIc. Comparison with the Pairwise Descreening Method. We also carried out similar tests on the related PDA approach to Born radii recently reported by Hawkins *et al.*[19] As noted in the Methods section, we found it advantageous to reoptimize their S_x based on our van der Waals radii and FDPB-derived $G'_{pol,i}$. We have compared the results with both the original (PDA, S_x parameters) and the revised (PDA*, S_x* parameters) parameter sets. The PDA and PDA* comparisons with FDPB $G'_{pol,i}$ are given in parts B and C of Figure 2. GB(PDA or PDA*) molecular solvation energies are compared with FDPB results and experiment in Figure 3C and Table 3.

For atomic solvent polarization energies and Born radii, the original PDA method provided a reasonable correlation with FDPB-derived results. However, using the reoptimized scaling factors (S_x*), PDA* performed significantly better relative to FDPB, especially with large molecules (Figure 2C). Statistics for these PDA and PDA* calculations are given in Table 2 and quantify the improvement in $G'_{pol,i}$ and α_i with the PDA* parameter set.

We then compared the G_{pol} from FDPB and GB(PDA) for 139 molecules in our data set that did not contain sulfur, phosphorus, or halogen. For the small molecules, PDA Born radii in conjunction with the GB equation yielded G_{pol} that are in good agreement with molecular FDPB results but systemati-

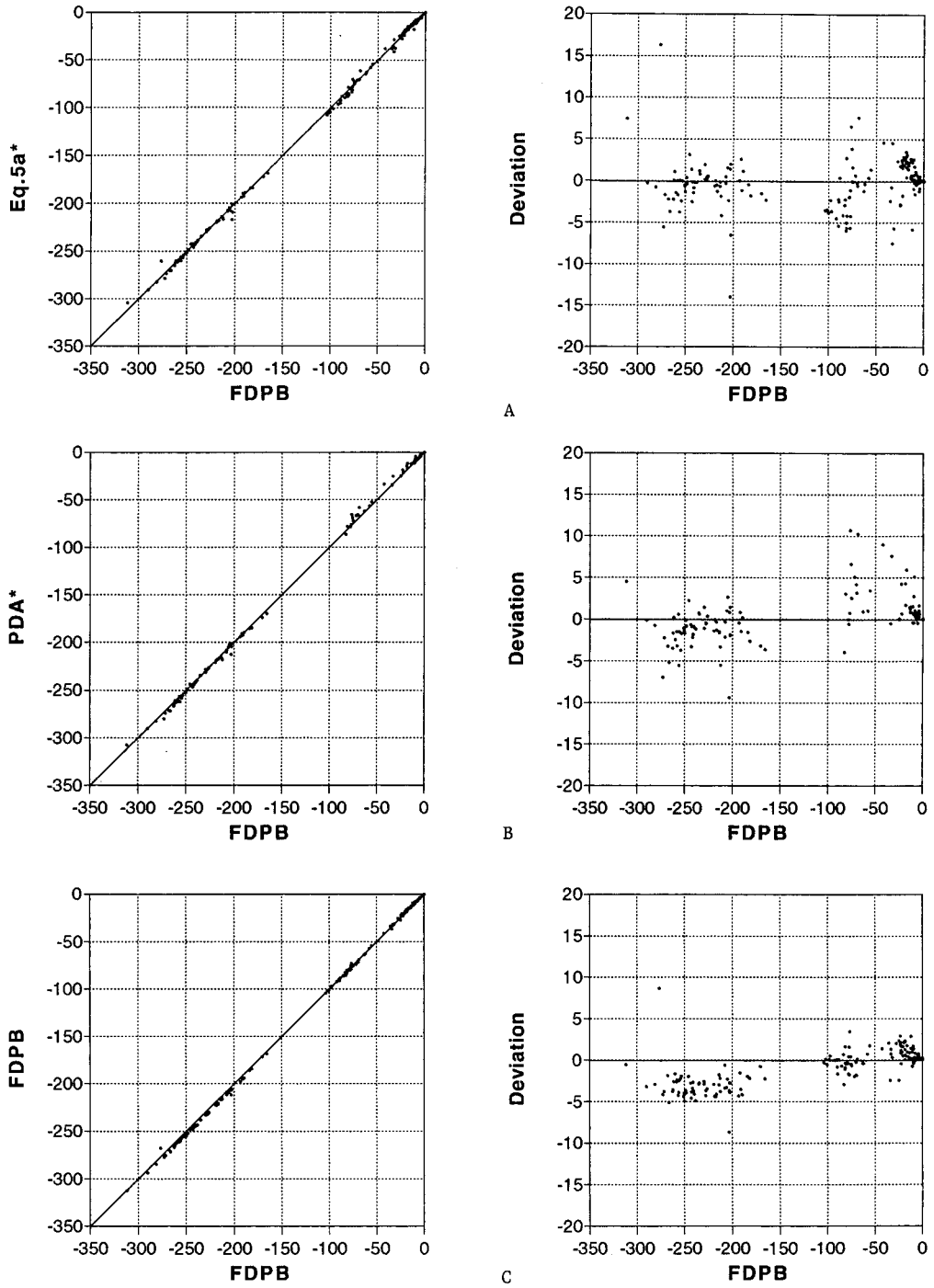

Figure 3. Comparison of molecular dielectric medium polarization energies (G_{pol}, kcal/mol) computed by the GB method using Born radii obtained by various methods. Panel A: GB radii from eq 5a with optimal atomic radii. Panel B: GB radii using the method of ref 19. Panel C: GB radii using method of ref 19 with reoptimized S_x parameters.

cally and significantly overestimate the FDPB energies for larger molecules (data not shown). Using PDA*, however, the larger molecules were brought back into line with only a small reduction in the goodness-of-fit for the small molecules. Overall, the GB(PDA*) G_{pol} energies were nicely correlated to accurate FDPB energies (linear slope = 1.012, r = 0.999) (Figure 3C). The average unsigned errors for such GB(PDA*) and GB(PDA) G_{pol} calculations are 1.84 and 10.19 kcal/mol. Finally, PDA and PDA* Born radii in the GB/SA calculations of hydration free energies of small molecules both give good correlations with experiment (average unsigned errors of 1.1 and 1.0 kcal/mol, respectively; see Table 3).

Overall, both the V/r^4 and the PDA (or PDA*) models provide valuable methods for rapidly computing useful, though approximate, Born radii. Relative to FDPB calculations for both large and small molecules, the V/r^4 model is marginally more accurate, although the effect of this on solvation free energies is probably negligible. Although the average unsigned error in reproducing observed solvation energies of small molecules is somewhat smaller with Born radii derived from our V/r^4 model (0.9 vs 1.0 kcal/mol), the precise solvation energies one calculates with the GB/SA solvation model vary with the choice of van der Waals radii and the source of atomic partial charges. Thus, the small differences in G_{sol} errors reported in Table 3 for the

TABLE 3: Comparision of Experimental Hydration Free Energies (G_{sol}, kcal/mol) and Those Calculated Continuum Solvation Models Using Various Born Radius Treatments

	GB/SA, Born radius source				FDPB/	
solute	eq 5a*	PDA	PDA*	FDPB	SA	expt
propane	1.8	1.9	1.8	1.8	1.9	2.0
n-butane	2.1	2.1	2.1	2.1	2.1	2.2
n-hexane	2.5	2.5	2.5	2.5	2.5	2.6
n-octane	2.9	2.9	2.9	2.9	2.9	2.9
2,4-dimethylpentane	2.8	2.8	2.8	2.8	2.8	2.9
cyclohexane	1.8	1.8	1.8	1.8	1.8	1.2
methanol	−7.3	−6.9	−6.6	−5.7	−6.7	−5.1
1-butanol	−5.0	−5.3	−4.8	−4.8	−5.6	−4.7
ethanol	−5.6	−5.9	−5.4	−5.2	−6.1	−5.0
2-propanol	−4.3	−4.7	−4.0	−4.2	−5.3	−4.8
1-hexanol	−4.6	−4.9	−4.3	−4.4	−5.2	−4.4
acetone	−2.7	−2.6	−2.3	−2.4	−2.3	−3.9
2-butanone	−2.0	−2.0	−1.6	−1.9	−2.0	−3.6
acetic acid	−6.4	−9.0	−7.9	−6.7	−7.0	−6.7
methyl acetate	−2.1	−2.6	−2.1	−1.9	−2.1	−3.3
dimethyl ether	−3.8	−1.9	−1.7	−1.9	−2.3	−1.9
benzaldehyde	−5.5	−6.1	−5.2	−5.4	−5.5	−4.0
acetonitrile	−4.7	−5.5	−5.3	−4.7	−4.6	−3.9
acetamide	−11.2	−12.6	−11.8	−11.5	−11.7	−9.7
dimethylamine	−2.3	−2.0	−1.8	−1.8	−2.7	−4.3
N-methylacetamide	−8.1	−8.6	−7.7	−8.1	−8.0	−10.1
N,*N*-dimethylacetamide	−5.7	−5.7	−5.1	−5.4	−5.5	−8.5
morpholine	−7.7	−5.7	−4.7	−6.5	−8.0	−7.2
ethyl mercaptan	−2.1	NA	NA	−2.0	−2.3	−1.2
methyl ethyl sulfide	−2.0	NA	NA	−1.9	−2.0	−1.4
thioanisole	−2.0	NA	NA	−2.2	−2.1	−2.7
thiophenol	−2.8	NA	NA	−3.0	−3.3	−2.6
benzene	−1.0	−1.2	−0.8	−1.0	−1.1	−0.9
phenol	−6.4	−7.5	−6.4	−6.4	−7.1	−6.6
aniline	−4.1	−6.9	−5.8	−5.7	−6.4	−4.9
naphthalene	−1.5	−1.6	−1.0	−1.6	−1.7	−2.4
o-xylene	1.0	1.0	1.3	1.0	1.0	−0.9
toluene	0.0	0.0	0.3	0.1	0.0	−0.8
pyridine	−4.2	−5.1	−4.3	−4.9	−4.9	−4.7
2-methylpyrazine	−5.0	−6.2	−5.1	−6.0	−6.0	−5.5
mean	−3.0	NA	NA	−2.9	−3.2	−3.2
av unsigned error	0.9	1.1	1.0	0.8	0.9	

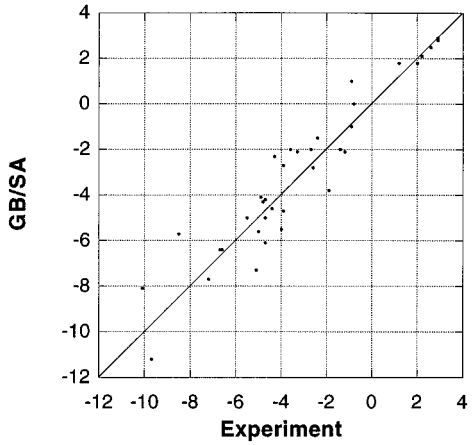

Figure 4. Comparision of experimental hydration free energies (G_{sol}, kcal/mol) and those calculated with the GB/SA method, using GB radii from eq 5a.

various methods of computing Born radii are unlikely to be significant.

Both the PDA and V/r^4 models are quite efficient. Computing the Born radii of all 10 034 atoms in our data set by these methods took 2.6 and 1.4 CPU seconds respectively on a 75 MHz Silicon Graphics workstation. Furthermore, since only the last term in eq 5a is coordinate dependent, the V/r^4 model would be even faster if Born radii were to be reevaluated with different molecular geometries. Our V/r^4 method is more rapid in part because the united-atom approximation for hydrocarbon portions of a solute (see Methods section) eliminates the need for considering the effects of hydrogen atoms.

IV. Conclusion

The simple analytical models described above for the Born radii calculation can have significant value in the rapid computation of solvation energies using the generalized Born (GB) continuum dielectric solvation model. Not only is the V/r^4 model for computing Born radii described here computationally efficient, but its accuracy in reproducing continuum dielectric polarization energies in the context of the GB model is comparable to that of classical but far more computationally intensive methods. The same can be said about the related PDA model for Born radii recently reported by Hawkins *et al.*[19]

We find it particularly telling that the GB solvation model with analytical Born radii reproduces the experimental solvation energies of small molecules in water essentially as accurately as the more elaborate Poisson−Boltzmann (PB) calculations. There are several possible reasons for this. One possibility is that solvation energy errors originating from surface-area-based atomic solvation parameters or inaccurate atomic partial charges or van der Waals radii outweigh the differences between the GB and PB treatments. Indeed, solvation energies can vary significantly when atomic partial charges are altered even slightly, and it is likely that more accurate charges will improve the performance of both the GB and PB methods. There is also the issue that the experimental hydration energies are not perfectly accurate and could easily be off by several tenths of a kilocalorie/mole. In addition, both models make arbitrary though differing assumptions about the precise shape of the cavity in which the solute is embedded. Another possibility, which we regard as more likely and significant, is that real water is only crudely described by a homogeneous continuum dielectric, especially near the solute−solvent interface. To make continuum solvation models perform much better than they do now, it may be necessary to treat solvent near the interface somewhat differently than solvent lying farther from the solute. Furthermore, the atomic partial charge model is simplistic in comparison with electrical properties of real molecules, and it may also need upgrading before highly accurate solvation energies are available by calculation.

Though the continuum solvation energies computed with analytical, approximate Born radii and the GB/SA model are far from perfect, they seem to model the effects of real solvation semiquantitatively and can be calculated quite rapidly. Furthermore, because the GB/SA continuum model is now fully analytical, derivatives of the energy with respect to atom movement are available and allow the effects of solvation to be included efficiently in energy minimization, molecular dynamics, etc. Such analytical first and second derivatives of the GB/SA solvation model have been a part of our molecular modeling program MacroModel for several years and, coupled with the newly parameterized V/r^4 model described here, should help to make molecular modeling in water a routine and more reliable affair.

Acknowledgment. This work was supported by NSF Grant CHE95 44253. We thank Shlomit Edinger of Professor R. Friesner's group for providing the nonapeptide structures.

Supporting Information Available: List of molecules and their 2D structures in the optimization data set, where the structures are minimized with MacroModel version 5.0 using

standard minimization techniques (13 pages). Ordering information is given on any current masthead page.

References and Notes

(1) Rossky, P. J.; Karplus, M. *J. Am. Chem. Soc.* **1979**, *101*, 1913.

(2) Jorgensen, W. L.; Chandrasekhar, J.; Madura, J. D.; Impey, R. W.; Klein, M. L. *J. Phys. Chem.* **1983**, *79*, 926.

(3) Jorgensen, W. L.; Ravimohan, C. J. *J. Chem. Phys.* **1985**, *83*, 3050.

(4) Eisenberg, D.; McLachlan, A. D. *Nature* **1986**, *319*, 199.

(5) Ooi, T.; Oobatake, M.; Nemethy, G.; Scheraga, H. A. *Proc. Natl. Acad. Sci. U.S.A.* **1987**, *84*, 3086.

(6) Kang, Y. K.; Nemethy, G.; Scheraga, H. A. *J. Phys. Chem.* **1987**, *91*, 4105, 4109, 4118.

(7) Warshel, A.; Russel, S. T. *Rev. Biophys.* **1984**, *17*, 283.

(8) Gilson, M.; Honig, B. *Proteins* **1988**, *4*, 7.

(9) Still, W. C.; Tempczyk, A.; Hawley, R. C.; Hendrickson, T. *J. Am. Chem. Soc.* **1990**, *112*, 6127.

(10) Cramer, C. J.; Truhlar, D. G. *J. Am. Chem. Soc.* **1991**, *113*, 8305.

(11) Hermann, R. B. *J. Phys. Chem.* **1972**, *76*, 2754.

(12) Amidon, G. L.; Yalkowsky, S. H.; Anik, S. T.; Valvani, S. C, *J. Phys. Chem.* **1975**, *72*, 2239.

(13) Floris, F.; Tomasi, J. *J. Comput. Chem.* **1989**, *10*, 616.

(14) Jayaram, B. *J. Phys. Chem.* **1994**, *98*, 5773.

(15) Nicholls, A.; Honig, B. *J. Comput. Chem.* **1991**, *12*, 435.

(16) Gilson, M.; Sharp, K. A.; Honig, B. *J. Comput. Chem.* **1988**, *9*, 327.

(17) Honig, B.; Nicholls, A. *Science* **1995**, *268*, 1144.

(18) Mohamadi, F.; Richards, N. G. I.; Guida, W. C.; Liskamp, R.; Lipton, M.; Caufield, C.; Chang, G.; Hendrickson, T.; Still, W. C. *J. Comput. Chem.* **1990**, *11*, 440.

(19) Hawkins, G. D.; Cramer, C. J.; Truhlar, D. G. *Chem. Phys. Lett.* **1995**, *246*, 122. This paper seems to contain a typographical error in one of the formulae, the correct formula is $U_{kk'} = R_{kk'} + \rho_{k'}$ if $\rho_k < R_{kk'} + \rho_{k'}$.

(20) Gilson, M. K.; Honig, B. *J. Comput.-Aided Molec. Des.* **1991**, *5*, 5.

(21) Jorgensen, W. L.; Tirado-Rives, J. *J. Am. Chem. Soc.* **1988**, *110*, 1657.

(22) Honig, B.; Sharp, K. A.; Yang, A. *J. Phys. Chem.* **1993**, *97*, 1101.

(23) Jean-Charles, A.; Nicholls, A.; Sharp, K.; Honig, B.; Tempczyk, A.; Hendrickson, T. F.; Still, W. C. *J. Am. Chem. Soc.* **1991**, *113*, 1454.

(24) Weiner, S. J.; Kollman, P. A.; Case, D. A.; Singh, U. C.; Chio, C.; Alagona, G.; Profeta, S.; Weier, P. J. *J. Am. Chem. Soc.* **1984**, *106*, 765.

(25) AMBER* force field has the same functional form and generally the same parameter set as AMBER.[24] For organic molecules having no specific AMBER parameters, functional-group-based parameters were assigned by analogy with corresponding peptidic side-chain functionality. Where no adequate analogy existed, partial atomic charges were developed by electrostatic potential (ESP) fitting of HF/6-31+G* wave functions, and torsional parameters were developed to reproduce HF/6-31+G* level conformational energies. For some peptides and carbohydrates, original AMBER parameters have been modified to better fit quantum mechanical data: a) McDonald, D. Q.; Still, W. C. *Tetrahedron Lett.* **1992**, *33*, 7743. (b) Senderowitz, H.; Parish, C.; Still, W. C. *J. Am. Chem. Soc.* **1996**, *118*, 2078. (c) McDonald, D. Q.; Still, W. C. *J. Org. Chem.* **1996**, *61*, 1385.

(26) Press, W. H.; Teukolsky, S. A.; Vetlerling, W. T.; Flannery, B. P. *Numerical Recipes in FORTRAN*; Cambridge University: Cambridge, 1992; p 436.

(27) Schaefer, M.; Froemmel, C. *J. Mol. Biol.* **1990**, *216*, 1045.

(28) Cramer, C. J.; Truhlar, D. G. *J. Comput.-Aided Molec. Des.* **1992**, *6*, 629.